Sound & Vibration 2025, 59(1), 2252.
https://doi.org/10.59400/sv2252

Article

The influence of metro operation vibration on single-layer cable net glass curtain wall structure based on frequency method

Zhirong Shen[1], Yuze Yan[1,*], Yi Tao[2], Zhiwei Wang[1]

[1] College of Civil Engineering, Tongji University, Shanghai 200092, China
[2] Shanghai Tongji Project Management & Consulting Co., Ltd., Shanghai 200092, China
*** Corresponding author:** Yuze Yan, 2232455@tongji.edu.cn

CITATION

Shen Z, Yan Y, Tao Y, Wang Z. The influence of metro operation vibration on single-layer cable net glass curtain wall structure based on frequency method. Sound & Vibration. 2025; 59(1): 2252. https://doi.org/10.59400/sv2252

ARTICLE INFO

Received: 20 December 2024
Accepted: 14 January 2025
Available online: 17 January 2025

Abstract: Using the single-layer cable net glass curtain wall of Siemens Shanghai Center Building A as a case study, the influence of vibrations from two metro lines on the structure was investigated through combination of field measurements with vibration signal analysis, and numerical simulations using finite element analysis. Time-domain data from cable vibrations were converted to frequency-domain data using fast Fourier transform for spectral analysis. The frequencies of the cables under different constraints were calculated based on the linear theory for vibrations of a string. A comprehensive numerical model of the single-layer cable net curtain wall was established for modal analysis. Comparative analysis shows that cables with horizontal floor constraints are highly vibration-sensitive, with metro operations causing high-order modal vibrations and fundamental frequency vibrations in sections between adjacent constraints, leading to glass deformation and damage. Neither metro operation induces the fundamental frequency vibration of the entire structure. Comparative frequency analysis favors theoretical frequency calculations with horizontal constraints for multi-constraint cable frequency analysis.

Keywords: metro operation; single-layer cable net glass curtain wall; frequency method; frequency domain analysis; finite element analysis

1. Introduction

In the field of architectural engineering, glass curtain walls are a widely used façade system due to their aesthetic appeal and functional benefits [1]. Among the various types of glass curtain walls, cable net systems have gained increasing popularity, especially in modern high-rise buildings [2]. These systems consist of a mesh of cables supporting glass panels, forming a flexible yet strong structure [3]. Single-layer cable net glass curtain walls, as a novel architectural façade system, are widely used in single-layer cable structures, with the supporting form typically being a single-layer planar cable net structure. Compared to traditional framed glass curtain walls, single-layer cable net glass curtain walls offer several advantages, such as lightweight construction, minimal material usage, and enhanced transparency [4]. Their high flexibility allows them to adapt to the dynamic loads they may encounter, making them suitable for large-scale and uniquely shaped structures [5]. However, the cable net system also has inherent limitations. Due to the tensioned nature of the cables, these systems are highly sensitive to external vibrations, which can lead to displacement or deformation under dynamic loading conditions [6]. For example, in urban environments where metro systems are prevalent, the vibration from underground transit can significantly affect the performance and safety of such systems [7]. In comparison to rigid-frame systems, cable net curtain walls are more

susceptible to this type of dynamic load, and their performance under these conditions requires further investigation.

The frequency method, a common approach for assessing cable tension and vibration in cable structures, has been widely used for various engineering applications [8]. This method involves measuring the natural frequencies of cables subjected to dynamic loads and using these frequencies, alongside theoretical formulations, to calculate the forces and vibrations within the cables [9]. Notable studies have demonstrated its effectiveness in evaluating the tension and fatigue of cables subjected to wind and traffic-induced vibrations. In the field of cable-stayed bridges and suspension bridges, the frequency method has been extensively applied for both testing and analysis of the cable behavior under dynamic conditions [10]. For cable-stayed bridges, the frequency method has been widely applied for both testing and analyzing the dynamic behavior of the cables. This method allows for precise measurement of the cable tension and monitoring of the structural integrity, particularly under varying load conditions such as wind and traffic-induced vibrations [11,12]. Similarly, in the case of suspension bridges, the frequency method has also proven to be an effective tool for investigating the dynamic behavior of the cables. Given the larger span and more flexible structure of suspension bridges, this method provides valuable insights into the interactions between the main cables, towers, and other components [13,14]. However, its application to cable net curtain walls, which involve more complex boundary conditions and dynamic interactions between the cables and glass panels, remains relatively scarce [15–17].

Recent advancements in the application of the frequency method to cable net structures have shown promise. For instance, studies have explored the effects of various environmental factors, such as wind, seismic activity, and impulsive loads, on the performance of these systems [18,19]. Additionally, numerical simulations combined with field measurements have allowed for more accurate predictions of cable behavior under dynamic loading conditions, such as seismic load effects [20,21] and wind load effects [22]. Previous studies have conducted full-scale experiments on certain panels of single-layer cable net curtain walls and investigated the cable prestress loss and cable anchorage end failure [23]. Other studies have shown that the glass panels have little impact on the lower-order vibration modes of the cable net curtain wall, but play a dominant role in the higher-order vibration modes and damping [24]. However, there is limited research on the overall dynamic characteristics of the curtain wall [25]. It is shown that metro trains are a source of increased noise and vibration, whose negative impact on residential development and production processes can lead to a deterioration in the quality of life or products [26]. Despite these advancements, the specific impact of metro-induced vibrations on the tensioned cables of single-layer cable net curtain walls, particularly in high-density urban areas, has not been sufficiently addressed in existing literature.

This study uses the single-layer cable net curtain wall of Building A at the Siemens Shanghai Center as a case study. Through combination of field measurements, theoretical analysis, and numerical simulations based on the frequency method, the true vibration behavior of the tensioned cables is obtained. The impact of metro operation-induced vibrations on the safety of the single-layer

cable net curtain wall of Building A is analyzed, providing valuable reference data for the design and testing of similar projects in the future.

2. Project overview

The Siemens Shanghai Center, completed in 2011, comprises three independent office buildings and a two-story restaurant with a waterfront landscape platform. Among these, Building A is the closest to the shared transfer hall of two metro lines. The southern façade, along with parts of the east and west facades of Building A, utilizes a single-layer cable net curtain wall system. The geographic location of Siemens Shanghai Center Building A and the spatial relationship between the intersection of Shanghai Metro Line 4 and Line 12 are illustrated in **Figure 1**.

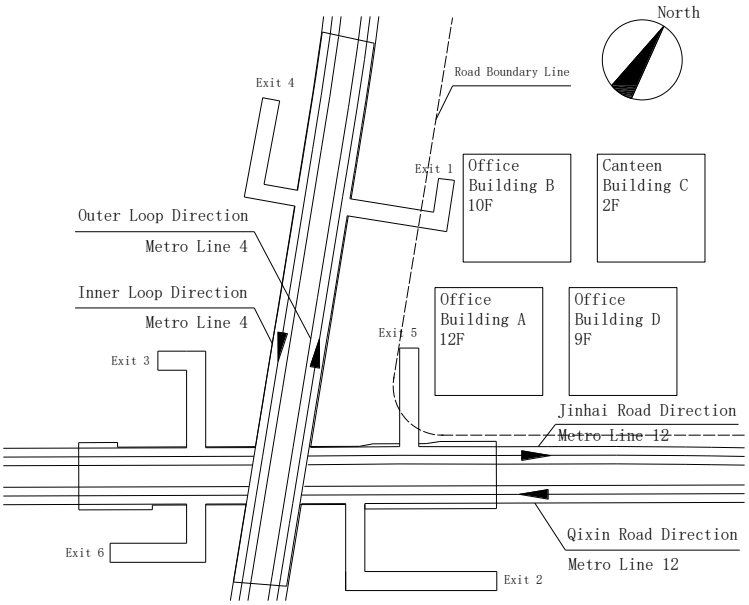

Figure 1. Floor plan schematic showing the relationship between Building A and the metro lines.

Metro Line 4, which opened in 2005, predates the completion of Building A. Metro Line 12, which opened in 2013, was established after Building A was constructed, and is positioned at a lower elevation compared to Line 4. The vibrations generated during the daily operation of these two metro lines have had a significant impact on the vibration-sensitive cable structure, leading to noticeable out-of-plane deformations of some of the curtain wall glass, as shown in **Figure 2**.

Building A consists of 12 floors, with the single-layer cable net curtain wall distributed from the 1st to the 9th floor. Each tensioned cable in the curtain wall system is equipped with a horizontal flat bar and a splicing claw at a height of 4 meters on the standard floors. Additionally, a splicing claw is installed at the center of the standard floor. On the ground floor and the 9th floor, two horizontal flat bars and splicing claws are arranged according to the structural load-bearing elements of the entrance revolving doors and main structural components. The horizontal flat bars and splicing claws directly bear the self-weight and wind loads of the curtain wall glass panels. This study selects six typical tensioned cables on the southern and

western façades of Building A, which are closest to the entrances of the metro interchange hall (the measurement points and numbering are shown in **Figure 3**. The aim is to investigate the vibration response of the single-layer cable net curtain wall structure under the influence of metro operation.

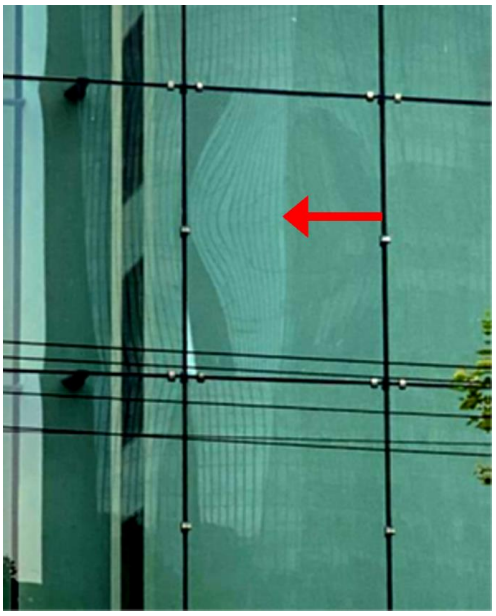

Figure 2. Out-of-plane deformation of glass panels (The glass panel highlighted by the red arrow shows substantial inward deformation, and the reflection pattern on the glass shows the deformation).

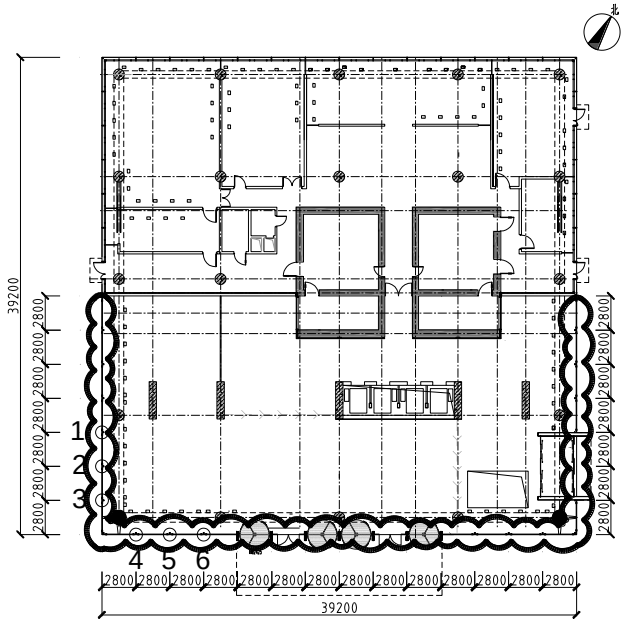

Figure 3. Measured layout diagram of cable placement points in Building A (Cloud line marking on the curtain wall area).

3. Tensioned cable field measurement and frequency analysis

The specifications and model numbers of the six tensioned cables measured on-site, as well as the initial pre-tension values applied, are identical to the design

values. The field measurements primarily include tests on the geometric and material parameters of the cables, tension degradation tests, free vibration tests, and vibration response tests of the cables during metro station entry and exit.

3.1. Geometric and material parameter testing of tensioned cables

A laser distance meter was used to measure the length of the cables, while a digital caliper was used to measure the cable diameter. All cables are made from Kin Long "Zn-5%Al-rare earth alloy coated" steel strands. The modulus of elasticity, unit mass per unit length, and cross-sectional area of the cables were based on data provided by the cable manufacturer. A summary of the measured geometric and material parameters of the cables are presented in **Table 1**.

Table 1. Geometry and material parameters of the cables.

Cable No.	Measured Length (m)	Measured Diameter (mm)	Effective Steel Stranding Area (mm^2)	Modulus of Elasticity (GPa)	Unit Mass per Unit Length (kg/100 m)
1	32.51	36.16	782	160	624
2	32.55	36.23	782	160	624
3	32.49	35.84	782	160	624
4	32.50	36.02	782	160	624
5	32.54	35.91	782	160	624
6	32.53	35.84	782	160	624

Note: In subsequent theoretical calculations and finite element modeling, the cable length is taken as the average measured length of 32.52 m, and the diameter is taken as the average measured diameter of 36.00 mm.

3.2. Tension degradation testing of tensioned cables

The design value for the tension of the tensioned cables is 330 kN. Over long-term service, the tension tends to degrade. Shanghai Construction Engineering Inspection Co., Ltd. has conducted quarterly monitoring of the tension in the cables of this single-layer cable net curtain wall [27]. The measurement points were located at the midpoints of two regions: the lower zone (elevation ±0.000 m to +5.120 m) and the upper zone (elevation +5.120 m to +9.120 m). The tension monitoring data for the six measured cables in June 2022 are shown in **Table 2**. The variation trends of the tension in all 27 cables of the single-layer cable net curtain wall over seven tests are illustrated in **Figure 4**.

Table 2. Tension monitoring data of the cables.

Cable No.	Design Value (kN)	Measured Value at Lower Zone (kN)	Remaining Tension Percentage	Measured Value at Higher Zone (kN)	Remaining Tension Percentage
1	330	301.2	91.27%	302.6	91.70%
2		302.1	91.55%	304.5	92.27%
3		299.7	90.82%	303.3	91.91%
4		286.1	86.70%	300.1	90.94%
5		304.3	92.21%	298.3	90.39%
6		303.1	91.85%	301.2	91.27%

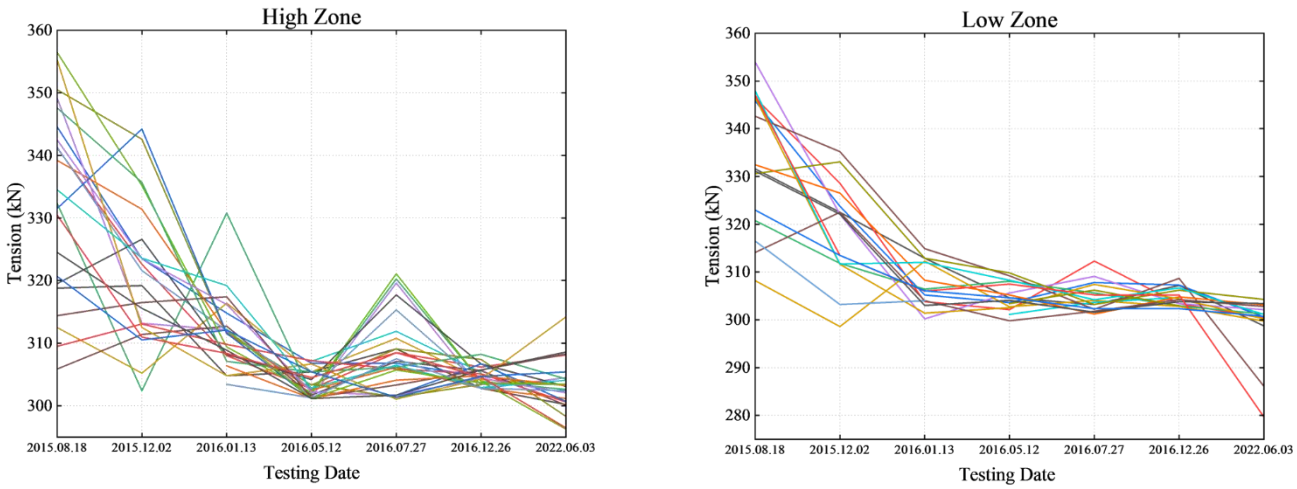

(a) **(b)**

Figure 4. Tension testing values at the high and low zone of the cables at different times. **(a)** High zone; **(b)** low zone.

The results indicate that the tension in the vast majority of the cables in the single-layer cable net curtain wall exhibited minimal variation during this monitoring period, with the maximum degradation being approximately 10%. The degradation trend appears to be stabilizing. However, a small number of cables, such as Cable 4 in the lower zone, exhibited significant tension degradation, reaching 13.3%, with an unstable degradation trend. This poses a substantial impact on the overall stability of the curtain wall structure.

3.3. Free vibration testing of tensioned cables

Due to the horizontal flat bar connected to the cable, if the constraint provided by the horizontal flat bar is considered and treated as a two-way hinged node, the entire tensioned cable can be divided into several cable segments. The length of the cable segment for the lower floor is 3 m, while the cable segment for the intermediate standard floors is 4 meters. Free vibration time history curves were measured for both the 3-meter and 4-meter cable segments of the six cables. The piezoelectric accelerometers used in the tests were of the type Lance LC0123T, with an integrated IC, and the measurement frequency range was 0.5 to 500 Hz. Data acquisition was carried out using the UA300 series 16-channel data logger, with data transmitted to the SVSA system for subsequent processing [28].

During the field measurements, the accelerometers were securely attached to the 3-meter cable segment on the ground floor and the 4-meter cable segment on the second floor. The cables were then excited manually, and the acceleration time history curves of the cable vibrations were recorded using the accelerometers and the SVSA system. The test setup is shown in **Figure 5**.

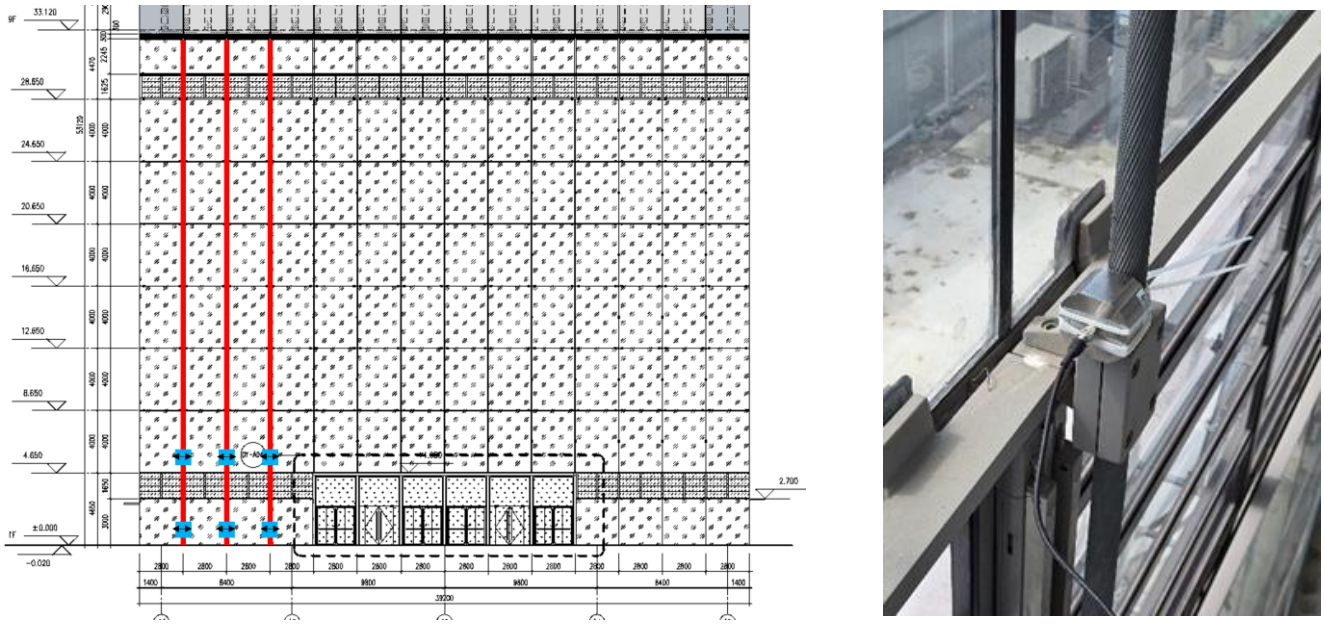

(a) **(b)**

Figure 5. Schematic diagram of accelerometer placement. **(a)** Schematic diagram of the sensor placement for Cable 4, 5, and 6 on the south facade. The red bold lines indicate the cables that were tested, the blue squares represent the accelerometers, and the black double arrows indicate the direction of vibration measurement; **(b)** real scene image of the accelerometer placement.

Figure 5 illustrates the sensor placement on the south facade, with the sensor arrangement on the west facade being similar. It is important to note that the sensors measured the horizontal vibration direction, which is also the direction most affected by external vibrations on the cables. The sensors were positioned at the lower end of the cable segment to avoid significant alteration of the mass distribution of the cables, which could potentially alter the natural frequency of vibration if placed at the middle. Although the amplitude of the measured vibration signals at the lower end is smaller than at the middle of the cable, the frequencies of the vibrations, which are the focus of this study, can be measured accurately at any point along the cable.

It should be noted that although the same measurement procedure was followed for all six cables during the vibration testing, due to space limitations in the paper, the results are only presented for Cable 2. The results of the 3-meter cable segment on the ground floor and the 4-meter cable segment on the second floor of Cable 2 are selected for display. The free vibration acceleration time history curves for Cable 2 are shown in **Figure 6**.

The figure clearly shows that after the cable is subjected to external excitation, the amplitude rapidly decays, which is consistent with the behavior of free vibration. The free vibration acceleration time history curves measured on-site were subjected to Fast Fourier Transform (FFT) using MATLAB software, converting the time domain data into the frequency domain. The resulting one-sided amplitude frequency spectra for the 3-meter cable segment and the 4-meter cable segment of Cable 2 across the full frequency range are shown in **Figure 7**.

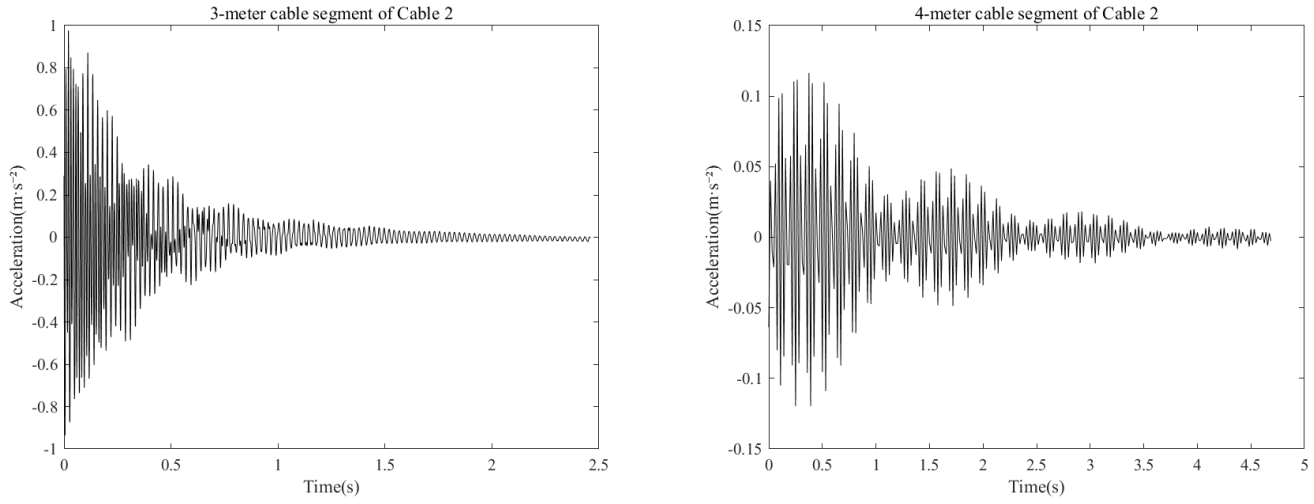

(a) **(b)**

Figure 6. Acceleration time history curves of the cable segments of Cable 2 during free vibration. **(a)** 3-meter cable segment; **(b)** 4-meter cable segment.

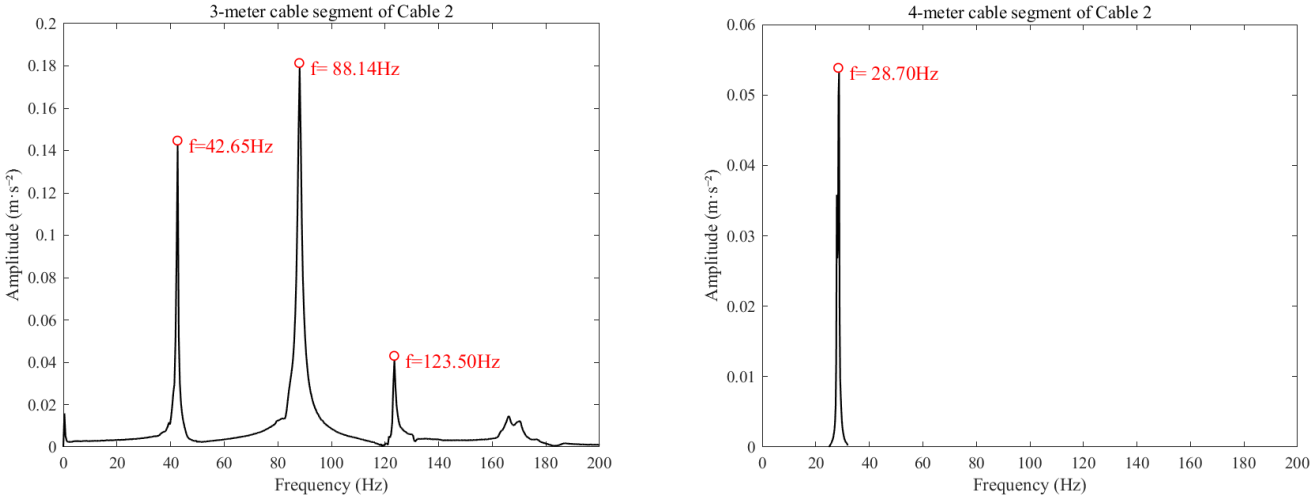

(a) **(b)**

Figure 7. Full-frequency amplitude-frequency spectrum of the cable segments of Cable 2. **(a)** 3-meter cable segment; **(b)** 4-meter cable segment.

The amplitude-frequency spectrum of the 3-meter cable segment exhibits three distinct peaks, and the corresponding frequency values approximately follow a harmonic relationship, which can be interpreted as the first to third-order natural frequencies of the 3-meter cable segment. Due to site constraints during the field measurements, the accelerometers could only be placed at the lower end of the cables, with the excitation point located approximately 1 meter from the lower end. As a result, multiple vibration modes may have occurred for the cable segments, which led to the appearance of multiple peaks in the amplitude frequency spectra, as shown in **Figure 7a**. In contrast, the amplitude-frequency spectrum of the 4-meter cable segment differs from that of the 3-meter segment, as it shows only one peak. This is likely due to the excitation point being located closer to the middle of the cable segment during the experiment, which only induced the first-order vibration of

the cable segment. The natural frequencies for the 3-meter and 4-meter cable segments of the six cables are shown in **Table 3**. When determining the natural frequencies in this case, the frequency corresponding to the first peak was taken as the natural frequency.

Table 3. Natural frequencies of each segment of the cable (Hz).

Cable No.	1	2	3	4	5	6
3 m segment	42.13	42.65	43.58	45.09	44.01	42.84
4 m segment	28.08	28.70	25.38	27.47	28.51	28.22

3.4. Vibration response testing of tensioned cables during metro station entry and exit

The vibration response acceleration time history curves of the six tensioned cables during the metro station entry and exit were measured. Similar to the free vibration tests, the accelerometers were securely attached to the 3-meter cable segment on the ground floor and the 4-meter cable segment on the second floor. Continuous and synchronized measurements were taken at the time points corresponding to the entry and exit of Metro Lines 4 and 12, with the excitation events being the station entry and exit. During this period, the acceleration time history curves of the cable vibrations were recorded using the vibration sensors and the SVSA system. The statistics for the metro entry and exit times for Lines 4 and 12 during the test period are presented in **Table 4**. The measured vibration acceleration time history curves for the 3-meter and 4-meter cable segments of Cable 2 during the metro entry and exit are shown in **Figure 8**.

To determine whether the collected signals indicate a significant external vibration source, the crest factor is defined by Equation (1) [29]:

$$Crest\ Factor = \frac{Maximum\ Peak\ Value}{Root\ Mean\ Square\ (RMS)\ Value} \tag{1}$$

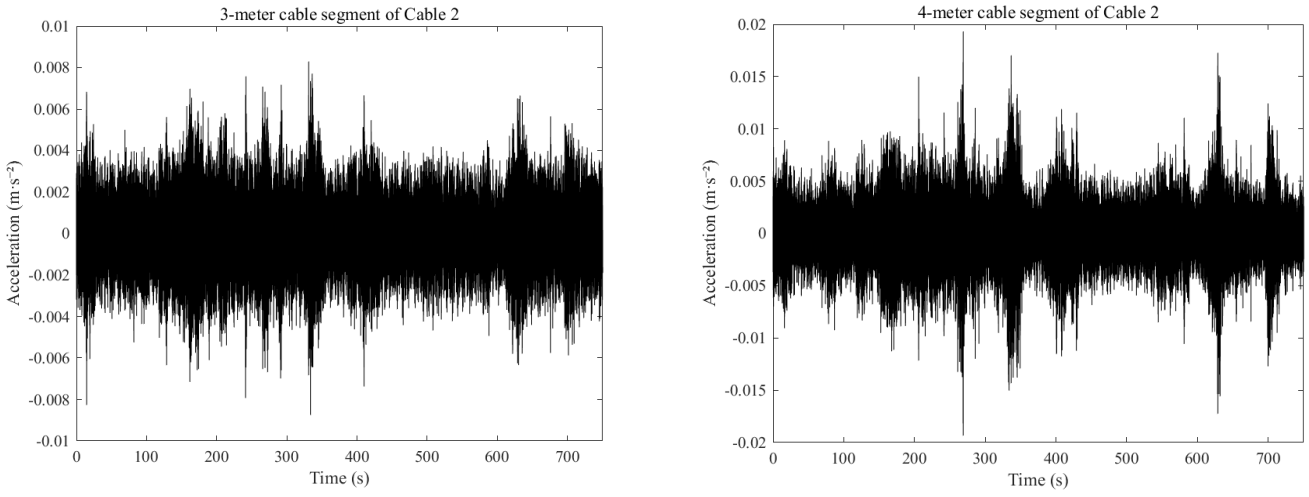

(a) **(b)**

Figure 8. Acceleration time history curves of the 3-meter cable segment of Cable 2 during metro entry and exit. **(a)** 3-meter cable segment; **(b)** 4-meter cable segment.

Table 4. Statistics of the entry and exit times for Metro Lines 4 and 12.

Status	Line 4 (Inner Loop direction)	Line 12 (Jinhai Road direction)	Line 4 (Outer Loop direction)	Line 12 (Qixin Road direction)
Entry and Exit 1	152 s~210 s	253 s~311 s	158 s~216 s	3 s~61 s
Entry and Exit 2	482 s~540 s	623 s~681 s	518 s~576 s	343 s~401 s
Entry and Exit 3	/	/	/	635 s~693 s

Note: Metro Line 4 is a circular line.

The crest factors for the acceleration time history curves of the 3-meter and 4-meter cable segments for the six measured cables are calculated and presented in **Table 5**.

Table 5. Crest factor of the acceleration time history curves of cable vibrations.

Cable No.	1	2	3	4	5	6
3 m segment	7.40	6.80	10.52	8.47	15.07	9.17
4 m segment	8.29	8.00	14.04	9.41	9.56	8.89

As seen in **Table 5**, the crest factors of the cable vibrations are generally large and concentrated around 7 to 9, with the crest factor of the 3-meter cable segment of Cable 5 even reaching 15.07. This indicates the presence of significant spike or impulse components in the signal, suggesting that the vibration response of the cables is notably influenced by external vibration. To further investigate, a frequency analysis of the entire signal duration was performed to understand the primary vibration frequencies of each cable during normal operation. The comparisons between the main operating frequencies and the measured natural frequencies for the six cables are shown in **Table 6**.

Table 6. Comparisons between the cable operating frequencies and the measured natural frequencies (Hz).

Cable No.	1	2	3	4	5	6
3 m Segment Operating Frequency	37.27	49.51	49.87	49.51	32.40	39.32
3 m Segment Natural Frequency	42.13	42.65	43.58	45.09	44.01	42.84
4 m Segment Operating Frequency	23.13	23.13	35.1	26.69	30	35.06
4 m Segment Natural Frequency	28.08	28.70	25.38	27.47	28.51	28.22

It can be observed that the operating frequencies for both the 3-meter and 4-meter cable segments are close to their respective natural frequencies, indicating that the cable segments primarily undergo fundamental mode vibrations during normal operation. The natural frequencies of most cable segments differ from their main operating frequencies by approximately 5 Hz. However, the main operating frequency of the 3-meter cable segment of Cable 5 is lower compared to the other cables. Additionally, as shown in **Table 4**, the crest factor of the vibration acceleration time history curve for the 3-meter segment of Cable 5 is very large, suggesting that it is more significantly affected by the vibrations caused by the metro operation. Therefore, it is necessary to extract the cable response time-domain

signals during the metro entry and exit periods to analyze the influence of metro operation vibrations on the cable vibration response. The amplitude-frequency spectrum for the 3-meter cable segment of Cable 5, corresponding to the Metro Line 12 (Jinhai Road direction) entry period, is shown in **Figure 9**.

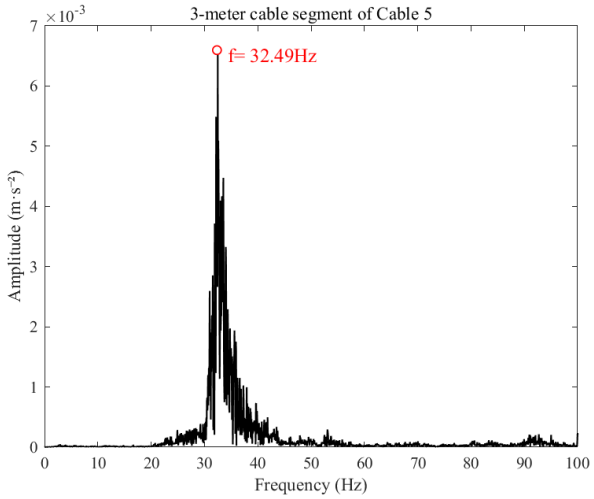

Figure 9. Full-frequency amplitude-frequency spectrum of the 3-meter cable segment of Cable 5.

It can be seen that the primary vibration frequency of Cable 5 during the extracted time period (32.49 Hz) is consistent with the main operating frequency for the entire duration (32.40 Hz), indicating that the entry and exit of Line 12 (Jinhai Road direction) are the main factors influencing the vibration of Cable 5. Since the Jinhai Road direction of Line 12 and the Outer Loop direction of Line 4 are closer to the single-layer cable net curtain wall of Building A, the cable vibration response is more pronounced. Therefore, only the effects of the entry and exit of these two directions are analyzed regarding their influence on the vibration response of the cables. The main vibration frequencies for the six cables during the entry and exit of both lines are shown in **Table 7**.

Table 7. Primary vibration frequencies of the cables for metro entry and exit on Line 12 (Jinhai Road direction) and Line 4 (Outer Loop direction) (Hz).

Cable No.		**1**	**2**	**3**	**4**	**5**	**6**
3 m segment	Line 12 (Jinhai Road direction)	33.52/45.55	49.64	44.81	35.57/41.2	32.49	34.03
	Line 4 (Outer Loop direction)	57.32	49.64/57.57	57.57	44.78/57.57	32.5/57.32	38.89/57.57
4 m segment	Line 12 (Jinhai Road direction)	35.35	35.35	28.33/34.7	35.35	35.35	35.14
	Line 4 (Outer Loop direction)	56.16	57.27	57.43	58.09	30.1/57.95	57.29

Note: The data before and after the "/" in the table represent the frequency values corresponding to the dual peak frequencies observed in the amplitude-frequency spectrum.

From **Table 7**, it can be observed that some cables (e.g., Cable 1) exhibit dual peak values in their power spectrum. One peak corresponds to the natural frequency of the cable, while the other peak corresponds to the vibration frequency induced by the metro operation. The vibration frequency range for metro Line 12 (Jinhai Road direction) during train entry and exit is between 32–35 Hz, and for metro Line 4

(Outer Loop direction), it is between 57–58 Hz. The vibration frequencies of the trains on Line 12 (Jinhai Road direction) are close to the natural frequencies of both the 3-meter and 4-meter cable segments, which could potentially cause the cable segments to undergo fundamental resonance.

Due to on-site coordination challenges, it was not possible to directly measure the metro vibration frequencies within the metro station. However, similar data can be found in the literature, which shows that the frequencies of metro-induced vibrations transmitted to adjacent buildings primarily range from 10 to 50 Hz [30]. This frequency range aligns with the metro vibration frequencies mentioned earlier, and the measured frequencies of the cables also fall within this range. This indicates that the external vibrations affecting the cables are indeed caused by the metro operation.

4. Theoretical and numerical simulation frequency analysis for the cables

4.1. Frequency calculation using string vibration frequency theories

The natural frequencies of the cables are calculated using existing theoretical formulas. The formula selection refers to the classical frequency calculation formulas for short cables that consider the bending stiffness of the cables [31], as well as the widely used suspension cable frequency calculation formulas in bridge engineering [32–34]. The fundamental principle behind these formulas is based on the linear theory for free vibrations of a string [35,36]. The anchoring devices at both ends of the cable are installed on the 1st and 9th floors of Building A. At the midpoint of the cable, several horizontal flat bar elements are distributed on the floors, connecting the entire cable system together. For a single cable, although the constraint effect of the horizontal flat bars is much weaker compared to the anchoring nodes at the top and bottom ends, considering the large sensitivity of the 32.52-meter-long cable to vibrations, especially in the sections with larger amplitudes at the midpoint, it is necessary to account for the constraint effect of the horizontal flat bars. Therefore, the following analysis is divided into two parts: one considering the cable without the horizontal flat bar constraint and the other considering the constraint effect in cable segments.

4.1.1. Frequency calculation ignoring horizontal constraints

If the constraint effects of the horizontal flat bars and curtain wall are ignored, the natural frequency of the cable can be calculated using the practical formula from the current Code for load testing of highway bridges [37]. The measured total cable length, unit length mass, and the most recent tension data are substituted into Equation (2) to calculate the natural frequencies:

$$f_n = \frac{n}{2l} \cdot \sqrt{\frac{T}{m}} \tag{2}$$

where: f_n—the n-th natural frequency of the cable;

n—the frequency mode number;

l—the total length of the cable;

T—the measured tension in the cable;

m—the unit length mass of the cable.

This equation is derived from the linear theory for the free vibrations of a string and has since been extended to include suspended cables and other types of tensioned cables. The result for the natural frequency of Cable 2 is shown in **Table 8**. Since the specifications of the cables are nearly identical, the frequency calculations for the other cables are very similar to that of Cable 2, but due to space limitations, they are not displayed here. Based on the earlier measured data, **Table 8** only focuses on the fundamental frequency and the 10th to 17th higher-order modes, while the frequencies of intermediate modes are omitted.

Table 8. Natural frequencies calculated by Equation (2) for cable 2 (Hz).

Mode	**1**	**…**	**10**	**11**	**12**	**13**	**14**	**15**	**16**	**17**
Frequency	3.38	…	33.83	37.21	40.6	43.98	47.36	50.75	54.13	57.51

As shown in **Table 8**, if the constraint from the horizontal flat bar on the cable is completely ignored, the first natural frequency of the cable is relatively low due to its large length, making it a highly sensitive structure in terms of vibration. The vibrations generated by the Line 12 (Jinhai Road direction) during train entry and exit primarily induce the 10th and 11th modes of vibration in the cable, while the vibrations from Line 4 (Outer Loop direction) mainly excite the 17th mode. For a single cable, without considering other constraints, external excitations are likely to induce higher-order vibrations. Moreover, due to the relatively low first natural frequency of the cable, variations in the external excitation frequency can also trigger vibrations in other modes. Generally speaking, the external excitations caused by train entry and exit are distributed within a certain frequency range. For the cables on Building A, it can lead to coupled vibrations of several higher-order modes.

4.1.2. Frequency calculation considering horizontal constraints

When considering the constraint from the horizontal flat bar, it is assumed to act as a bidirectional hinge. The lower cable section corresponds to a length of 3 meters, while the standard middle layers correspond to a cable section length of 4 meters. If both the horizontal flat bar constraint and the constraint from a single connecting clamp at the center of each standard layer are considered, each cable section of standard layer can be subdivided into two 2-meter smaller cable segments. The frequencies of these three types of cable segments are analyzed separately below. Since the cable segments are relatively short, it is necessary to account for the bending stiffness and boundary conditions, which require modifications to the formula. The natural frequencies of the cable segments are calculated according to Equation (3) [38]:

$$f_1 = \frac{1}{2l} \cdot \sqrt{\frac{T}{m}} + \frac{1.182}{l^2} \cdot \sqrt{\frac{EI}{m}} \tag{3}$$

where: f_1—the fundamental natural frequency of the cable;

l—the length of the cable segment;

T—the measured tension in the cable;
m—the unit length mass of the cable;
E—modulus of elasticity of the cable material;
I—the moment of inertia of the cable cross-section.

This formula takes into account the basic parameters of the cable, as well as the bending stiffness of the cable, making it particularly effective for calculating the natural frequency of short cables. It is well-suited to the cable segments discussed in this study. The calculated natural frequencies of the cable segments for Cable 2 are shown in **Table 9**. The natural frequencies of the other cable segments are similar to those of Cable 2.

Table 9. Self-resonant frequencies calculated by modified string theory for segments of Cable 2 (Hz).

Length of Cable Segment	**2 m**	**3 m**	**4 m**
Calculated Frequency	66.92	41.96	30.48
Measured Frequency	/	42.55	28.57

From **Table 9**, it can be observed that the calculated natural frequencies of the 3-meter and 4-meter cable segments match closely with the measured natural frequencies. Additionally, the calculated natural frequency of the 2-meter cable segment corresponding to the standard layer is 67 Hz, which is close to the excitation frequency range of 57–58 Hz from the Metro Line 4 (Outer Loop direction), indicating that the train entry and exit from Line 4 are likely to induce resonance in this cable segment. The 4-meter cable segment natural frequency of 30.48 Hz is close to the excitation frequency range of 32–35 Hz from the Metro Line 12 (Jinhai Road direction), suggesting that the train entry and exit from Line 12 are likely to induce resonance in the central cable segment. In addition, the maximum amplitude of this vibration occurs at the middle of the 4-meter cable segment, where a single anchoring claw is located. Large vibrations at the anchoring claw could lead to deformations in the glass curtain wall.

4.2. Numerical simulation of frequency calculation

4.2.1. Model overview

Based on the structural drawings of the single-layer cable net curtain wall of Building A and filed measured data, an overall finite element model of the single-layer cable net curtain wall was constructed using SAP2000 software. In the model, the 27 cables forming the curtain wall structure all have the same specifications. These cables are modeled as beam elements with circular cross-sections, whose moments of inertia are reduced to 10% of the actual value (further reduction has negligible impact on the results), in order to eliminate the bending stiffness of the beam elements and simulate the behavior of the cables. The anchoring claws are modeled using beam elements with the same cross-sectional area as the horizontal flat bars. The glass panels are modeled using shell elements, considering the in-plane stiffness of the panels. Hinged supports are used at both ends of each cable. For each horizontal flat bar, the moment is released at both ends along the three axes, so that

the connection nodes between the flat bars are treated as hinges, which aligns with the actual configuration. For the purpose of modal frequency analysis, no external loads such as wind loads are considered. Only the self-weight loads of the cables, horizontal flat bars, and glass panels are included. The cable tension is applied by setting an initial strain corresponding to the measured tension of 300 kN, which results in a total applied strain of 0.00263, applied at the top of the cables. A schematic diagram of the overall model calculation is shown in **Figure 10**.

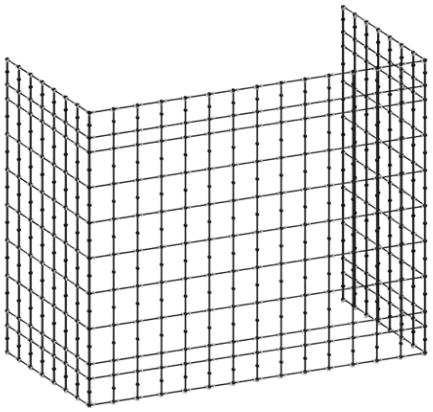

Figure 10. Schematic diagram of the overall model calculation.

In the numerical simulation, both the node stiffness and damping of the connection nodes between the flat bars were set to zero, effectively modeling the nodes as simple hinge connections. This assumption was based on site inspections and a review of the structural drawings, which revealed that the connection nodes are only fastened with bolts and simple connecting components, without any stiffening ribs or welded connections that would provide significant stiffness. As a result, the nodes were simplified as hinge connections. Furthermore, the simulation results obtained with this assumption were found to be in good agreement with the measured results, validating the effectiveness of this simplification in the model.

4.2.2. Comparison of simulation results

In the numerical simulation, the self-weight load of the glass curtain wall is jointly carried by the horizontal flat bars at the bottom of the curtain wall and the anchoring claws located at the center of the panels. The cable tension decreases monotonically from the upper to the lower parts of the cables. The simulation results show that the cable tension at the upper anchoring node is 356.78 kN, while at the lower anchoring node, it is 302.45 kN. The measured cable tension at the lower anchoring node is approximately 300 kN, which is in close agreement with the numerical simulation results, indicating that the simulation results are in good alignment with the actual conditions.

The vibration mode periods and frequencies of the cables in the simulation also require careful attention. Through modal analysis in the numerical simulation, the first three modal shapes of the single-layer cable net curtain wall are obtained. These modes are shown in **Figure 11**.

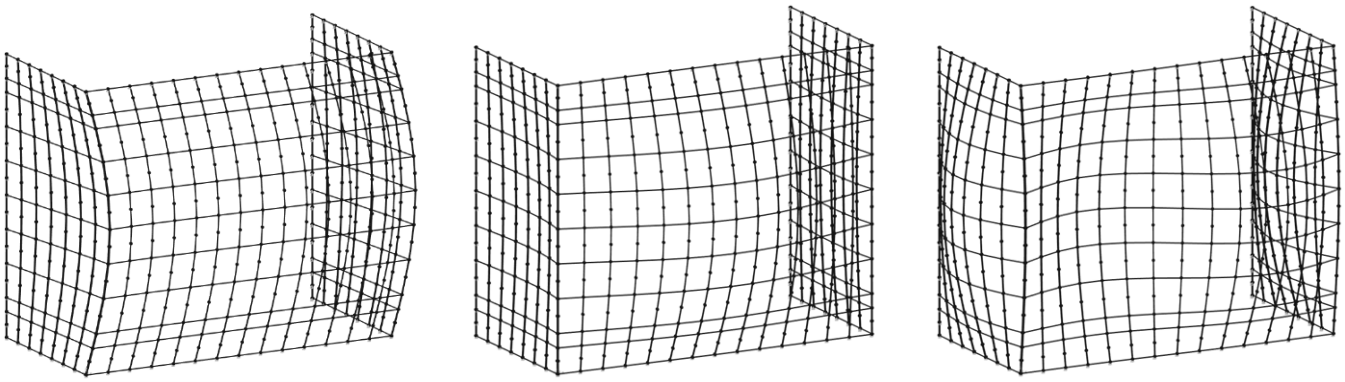

(a) **(b)** **(c)**

Figure 11. Vibration modes of the single-layer cable net curtain wall. **(a)** 1st-order vibration mode, f_1 = 3.01 Hz; **(b)** 2nd-order vibration mode, f_2 = 3.04 Hz; **(c)** 3rd-order vibration mode, f_3 = 3.15 Hz.

It can be seen from **Figure 11** that the overall structure of the curtain wall is highly sensitive to vibrations, with several low-order modes that have similar frequencies, all around 3 Hz. The overall natural frequency of the single-layer cable net curtain wall is close to the fundamental frequency of the entire cable, which is 3.38 Hz. However, during the actual operation of the cables, the external excitation frequencies from the metro lines during train entry and exit are mainly concentrated in the 32–35 Hz and 57–58 Hz ranges, which are unlikely to cause resonance at the fundamental frequency of the entire curtain wall.

Further calculations of the higher-order modes of the curtain wall show that the frequencies of the 518th and 746th modes (shown in **Figure 12**) correspond to the excitation frequencies from the Metro Line 12 (Jinhai Road direction) and Line 4 (Outer Loop direction), respectively. These mode frequencies fall within the frequency ranges of the external excitation caused by metro operation. Moreover, from the mode shapes, it can be observed that the cable segments between the horizontal flat bars undergo low-order vibrations, indicating that this vibration results from the coupling between the high-order vibration modes of the curtain wall and the fundamental frequency vibration of the cable segments between the horizontal flat bars.

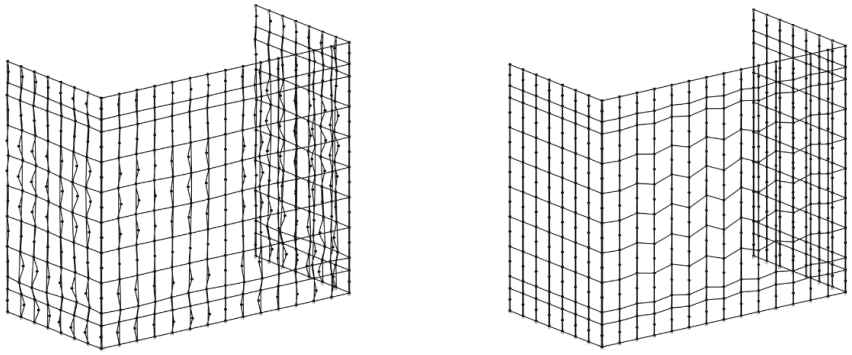

(a) **(b)**

Figure 12. High-order vibration modes of the single-layer cable net curtain wall at metro excitation frequencies. **(a)** 518th-order vibration mode, f_{518} = 35.32 Hz; **(b)** 746th-order vibration mode, f_{746} = 58.21 Hz.

5. Discussion

5.1. Comparison of frequency analysis methods

The comparison of the results from the theoretical formulas and numerical simulations for the calculation of the cable natural frequencies reveals that the theoretical formulas are more focused on the natural frequencies of smaller segments of the cables, while the numerical simulations emphasize the overall natural frequency of the single-layer cable net curtain wall. When comparing the measured frequencies with those calculated using the theoretical methods, it is observed that the frequencies obtained from the theoretical analysis considering horizontal constraints are close to the measured frequencies. On the other hand, the low-order natural frequency obtained from the overall modeling of the single-layer cable net curtain wall differs significantly from the measured frequencies. Through numerical simulations, obtaining higher-order natural frequencies is theoretically feasible. However, in practice, this approach has certain limitations. Firstly, the efficiency is relatively low, as calculating hundreds of vibration modes requires substantial computational resources. Secondly, it is difficult to determine the specific resonating modes due to external vibrations. As a result, the efficiency and accuracy of this method still require improvement. Therefore, in the context of this study, the frequency analysis method considering multi-horizontal constraints is a better approach for frequency analysis.

5.2. Discrepancy in experimental data

During the field measurements, there may be some discrepancy in the data collected for different cables. For free vibration testing of cables, the location of the external excitation plays a crucial role in the results. If the excitation is applied near the middle of the cable segment, it is more likely to induce resonant vibrations at the fundamental frequency of the segment. Conversely, if the excitation is closer to the ends of the cable segment, higher-order coupling vibrations are more likely to occur, resulting in a multi-peak phenomenon in the amplitude-frequency spectrum, as demonstrated in the results shown in **Figure 7**. For vibration testing of cables during metro train entry and exit, there are multiple factors contributing to the differences in cable frequencies. These include variations in the position of the cable, as well as structural differences such as the condition of the anchoring nodes and the connection points of the horizontal flat bars, all of which can influence the cable's vibration frequency.

When calculating the frequencies using theoretical formulas and numerical simulations, slight discrepancies with the measured data may still occur, especially for lower-order modes. In addition to the structural differences in the cables and associated components mentioned above, these discrepancies also arise from the simplification of the cable's end anchorage nodes and the horizontal flat bar connection nodes. In this study, both types of nodes were simplified as hinge supports. However, in reality, the nodes should be considered as having a stiffness between rigid and hinged supports. From the results, it can be seen that the use of hinged supports for simulation yields better agreement with the measured data. In

future research, the nodes could be assigned specific stiffness and damping coefficients to more accurately simulate the fixed effects of the nodes. Additionally, the presence of environmental factors, such as ambient noise and vibrations from external sources, could have influenced the measurements. These factors are often difficult to control in field tests, which could lead to discrepancies between the theoretical and measured results.

Furthermore, due to the limited amount of cable monitoring data in this study, the potential fatigue damage caused by the long-term effects of metro vibrations on the cables has not been considered. The fatigue behavior of single-layer cable nets has been studied using the cumulative damage theory [39], and demonstrated that the fatigue life of single-layer cable net curtain walls can be significantly shortened in the presence of strong external vibration sources, such as wind-induced vibrations. Metro operations are periodic, with vibrations generated each time trains enter or exit stations, which aligns with the definition of cyclic loading that is prone to inducing fatigue damage. For cables, which are prestressed structures, the consequences of fatigue damage go beyond the loss of prestress, leading to gradual structural failure. More critically, fatigue damage could also affect the associated structures of the cable, such as the failure due to bolt loosening or weld failure in the horizontal flat bar connection nodes. Therefore, the study of cable fatigue damage is essential. In future research, long-term monitoring of metro operational vibrations could be conducted, and a model of this vibration source could be developed to simulate the fatigue life of the cables.

5.3. Engineering application to different curtain wall structures

Based on the findings of this study, it is evident that different types of curtain wall structures, such as single-layer cable net curtain walls and frame-glass curtain walls, exhibit varying responses to operational vibrations in metro environments. In light of these findings, it is crucial to establish tailored strategies for the application of different curtain wall designs in environments subject to significant vibration, such as those encountered in metro stations.

The cable net curtain wall structure exhibits favorable dynamic characteristics when subjected to large-amplitude vibrations, such as those induced by seismic events. However, when exposed to cyclical, low-amplitude vibrations, as experienced in metro operations, the stress relaxation phenomenon in the cables becomes a significant weakness of the system. This cyclical loading, characteristic of the repetitive entry and exit of metro trains, induces long-term fatigue damage, leading to a gradual loss of prestress in the cables, which in turn compromises the structural integrity and overall performance of the curtain wall. For environments with high vibrational exposure, it may be necessary to optimize curtain wall designs to enhance their vibration resilience. This could include incorporating additional damping measures, selecting materials with improved vibration resistance, or adopting alternative structural forms that are less susceptible to resonance under the operational frequencies of nearby metro lines. For instance, in single-layer cable net curtain walls, enhancing the structural connectivity and flexibility of the design could mitigate the risk of excessive deformation, while for frame-glass curtain walls,

incorporating shock-absorbing elements at critical points of connection could prove beneficial.

Moreover, the frequency analysis methods utilized in this study—particularly the consideration of multi-horizontal constraints—can be extended to other curtain wall structures facing similar operational challenges. This theoretical calculation method offers a cost-effective and efficient means to conduct preemptive vibration risk assessments, which can provide essential insights into potential resonance and fatigue issues. Meanwhile, numerical simulation remains a robust and precise validation method. With its high accuracy, it serves as an effective tool for comparing experimental data with theoretical calculations, thereby further enhancing the validity of the results. By applying the frequency analysis techniques developed in this research, engineers can more accurately evaluate the dynamic behavior of curtain wall systems and develop targeted design interventions to ensure the longevity and safety of the structure in high-vibration environments.

In conclusion, the practical application of the study's findings could be extended beyond the single-layer cable net curtain wall, offering a valuable approach for the design and optimization of curtain wall systems in other high-vibration settings, such as transportation hubs and industrial facilities. By integrating these advanced vibration analysis methodologies, engineers can more effectively address the dynamic challenges posed by metro environments, ensuring that curtain wall systems maintain their structural integrity over time.

6. Conclusion

Based on the research, the following conclusions can be drawn:

a) Due to the constraint effect of the horizontal flat bars, the overall vibration of the cables is mainly composed of the fundamental frequency vibration of the cable segments between the horizontal flat bars. The theoretical values of the natural frequencies for the 3-meter and 4-meter cable segments match the measured values, verifying the validity and accuracy of the theoretical results.

b) The excitation caused by the Metro Line 12 (Jinhai Road direction) during train entry and exit is likely to induce the fundamental frequency vibration of both the 3-meter and 4-meter cable segments. From the overall numerical simulation results of the single-layer cable net curtain wall, it can also excite higher-order mode vibrations of the curtain wall. Therefore, under this excitation, the cables are prone to complex coupled vibration responses. Long-term exposure to this excitation will not only cause the loosening of the cable tension but also result in excessive deformation of the horizontal flat bars connected to the cables, which is the primary cause of the deformation of the glass curtain wall.

c) The excitation frequency from the Metro Line 4 (Outer Loop direction) during train entry and exit induces the fundamental frequency vibration of the 2-meter cable segment, which has a minimal effect on the glass curtain wall. The excitation from both metro lines is unlikely to cause resonance at the overall fundamental frequency of the single-layer cable net curtain wall structure.

d) When calculating the dynamic characteristics of the single-layer cable net curtain wall cables under metro operational vibrations, considering the multi-

horizontal constraints in the theoretical frequency analysis method is more efficient and accurate than using an overall numerical model for frequency calculation.

Author contributions: Conceptualization, ZS; methodology, ZS and YY; data curation, YY and ZW; formal analysis, YY; investigation, YY and ZW; validation, YY and ZW; writing—original draft preparation, YY; writing—review and editing, ZS and YT; supervision, ZS and YT; project administration, YT. All authors have read and agreed to the published version of the manuscript.

Acknowledgments: The authors would like to express their gratitude to the editors and anonymous reviewers for their and suggestions. Additionally, the client of this project, Siemens (China) Ltd., has expressed strong satisfaction with the outcomes of this research. They regard the results and recommendations as highly reliable and have acknowledged that single-layer cable net curtain walls are not suitable for environments with significant vibrations from metro operations. In response to these findings, the client has already initiated the reconstruction of the curtain wall structure for Building A of the Siemens Shanghai Center in the second half of 2024.

Conflict of interest: The authors declare no conflict of interest.

References

1. Feng C, Ma F, Wang R, et al. An experimental study on the performance of new glass curtain wall system in different seasons. Building and Environment. 2022; 219: 109222. doi: 10.1016/j.buildenv.2022.109222
2. Kunaratnam J. Behaviors of the Curtain Wall Facade in the Tall Building Under Dynamic Actions-An Overview and Recommendations. Advances in Technology. 2023; 33-39.
3. Feng RQ, Wu Y, Shen SZ. Working Mechanism of Single-Layer Cable Net Supported Glass Curtain Walls. Advances in Structural Engineering. 2007; 10(2): 183-195. doi: 10.1260/136943307780429734
4. Yussof M. Cable-net supported glass facade systems [PhD thesis]. University of Surrey; 2015.
5. Yang B, Zhu H, Wüchner R, et al. Monitoring of wind effects on a wind-sensitive hybrid structure with single-layer cable-net curtain walls under Typhoon Muifa. Journal of Building Engineering. 2021; 44: 102960. doi: 10.1016/j.jobe.2021.102960
6. Behr RA, Belarbi A, Culp JH. Dynamic racking tests of curtain wall glass elements with in-plane and out-of-plane motions. Earthquake Engineering & Structural Dynamics. 1995; 24(1): 1-14. doi: 10.1002/eqe.4290240102
7. Tao Z, Zou C, Wang Y, et al. Vibration transmissions and predictions within low-rise buildings above throat area in the metro depot. Journal of Vibration and Control. 2021; 29(5-6): 1105-1116. doi: 10.1177/10775463211057644
8. Kim BH, Park T. Estimation of cable tension force using the frequency-based system identification method. Journal of Sound and Vibration. 2007; 304(3-5): 660-676. doi: 10.1016/j.jsv.2007.03.012
9. Yan B, Yu J, Soliman M, et al. Estimation of cable tension force independent of complex boundary conditions. Journal of Engineering Mechanics. 2015; 141(1): 06014015. doi: 10.1061/(ASCE)EM.1943-7889.0000836
10. Bao Y, Shi Z, Beck JL, et al. Identification of time-varying cable tension forces based on adaptive sparse time-frequency analysis of cable vibrations. Structural Control and Health Monitoring. 2016; 24(3): e1889. doi: 10.1002/stc.1889
11. Li YQ, Zhao HW, Yue ZX, et al. Real-Time Intelligent Prediction Method of Cable's Fundamental Frequency for Intelligent Maintenance of Cable-Stayed Bridges. Sustainability. 2023; 15(5): 4086. doi: 10.3390/su15054086
12. Zeng Y, Zheng H, Jiang Y, et al. Modal Analysis of a Steel Truss Girder Cable-Stayed Bridge with Single Tower and Single Cable Plane. Applied Sciences. 2022; 12(15): 7627. doi: 10.3390/app12157627
13. Petersen ØW, Øiseth O, Lourens E. Investigation of dynamic wind loads on a long-span suspension bridge identified from measured acceleration data. Journal of Wind Engineering and Industrial Aerodynamics. 2020; 196: 104045. doi: 10.1016/j.jweia.2019.104045

14. Guo J, Hu CJ, Zhu MJ, et al. Monitoring-based evaluation of dynamic characteristics of a long span suspension bridge under typhoons. Journal of Civil Structural Health Monitoring. 2021; 11(2): 397-410. doi: 10.1007/s13349-020-00458-5
15. Xia J, Yao Y, Wu X, et al. Cable Force Measurement Technology and Engineering Application. Journal of the International Association for Shell and Spatial Structures. 2021; 62(3): 185-194. doi: 10.20898/j.iass.2021.006
16. Li S, Chen S. Field monitoring and prediction on temperature distribution of glass curtain walls of a super high-rise building. Engineering Structures. 2022; 250: 113405. doi: 10.1016/j.engstruct.2021.113405
17. Xu D, Wang Y, Xie J. Monitoring and Analysis of building curtain wall deformation based on optical fiber sensing technology. Iranian Journal of Science and Technology, Transactions of Civil Engineering. 2022; 46: 3081-3091. doi: 10.1007/s40996-021-00735-3
18. Momeni M, Bedon C. Review on Glass Curtain Walls under Different Dynamic Mechanical Loads: Regulations, Experimental Methods and Numerical Tools. In: Bedon C, Kozlowski M, Stepinac M, Haddad A (editors). Façade Design—Challenges and Future Perspective. IntechOpen; 2024.
19. Zhou Q, Lu W, Peng X, et al. Frequency calculation method and wind-induced dynamic response of cable net façades considering the façade stiffness. Structures. 2023; 55: 718-726. doi: 10.1016/j.istruc.2023.06.070
20. Aiello C, Caterino N, Maddaloni G, et al. Experimental and numerical investigation of cyclic response of a glass curtain wall for seismic performance assessment. Construction and Building Materials. 2018; 187: 596-609. doi: 10.1016/j.conbuildmat.2018.07.237
21. Li J. Vibration response test method of curtain wall under seismic coupling. Arabian Journal of Geosciences. 2021; 14(6). doi: 10.1007/s12517-021-06849-2
22. Bakhtiari A, Alawode KJ, Vutukuru KS, et al. Wind-Induced Dynamic Behavior of Single-Skin Curtain-Wall System: A Comparative Numerical Study. Journal of Architectural Engineering. 2024; 30(4). doi: 10.1061/jaeied.aeeng-1725
23. Shi G, Zuo Y, Shi X, et al. Influence of damages on static behavior of single-layer cable net supported glass curtain wall: full-scale model test. Frontiers of Architecture and Civil Engineering in China. 2010; 4(3): 383-395. doi: 10.1007/s11709-010-0074-6
24. Feng R, Zhang L, Wu Y, et al. Dynamic performance of cable net facades. Journal of Constructional Steel Research. 2009; 65(12): 2217-2227. doi: 10.1016/j.jcsr.2009.06.020
25. Xu G, Chen G. Simulation Study on vibration frequency of monolayer cable net glass curtain wall. In: Khalil R, Yang J (editors). Advances in Urban Engineering and Management Science Volume 1, 1st ed. CRC Press; 2022. pp. 338-343.
26. Mondrus V, Sizov D, Dashevskij M, Mitroshin V. Impact of metro induced ground-borne vibration on urban development. Magazine of Civil Engineering. 2021; 6(106): 10602. doi: 10.34910/MCE.106.2
27. Shanghai Construction Engineering Inspection Co., Ltd. Tension testing report of point-cable glass curtain wall in Building A of Siemens Shanghai Center. Shanghai Construction Engineering Inspection Co., Ltd. 2017.
28. Xu HM, Li YY, Xu W. Dynamic Characteristic Analysis of Prefabricated Houses of Light-Weight Steel Structure. Applied Mechanics and Materials. 2014; 578-579: 483-487. doi: 10.4028/www.scientific.net/amm.578-579.483
29. Harris C, Piersol AG. Harris' shock and vibration handbook. New York: McGraw-Hill; 2002.
30. Zou C, Wang Y, Wang P, et al. Measurement of ground and nearby building vibration and noise induced by trains in a metro depot. Science of The Total Environment. 2015; 536: 761-773. doi: 10.1016/j.scitotenv.2015.07.123
31. Ceballos MA, Prato CA. Determination of the axial force on stay cables accounting for their bending stiffness and rotational end restraints by free vibration tests. Journal of Sound and Vibration. 2008; 317(1-2): 127-141. doi: 10.1016/j.jsv.2008.02.048
32. Duan YF, Wu SK, Wang SM, et al. Train-Induced Dynamic Behavior and Fatigue Analysis of Cable Hangers for a Tied-Arch Bridge Based on Vector Form Intrinsic Finite Element. International Journal of Structural Stability and Dynamics. 2022; 22(12). doi: 10.1142/s021945542250136x
33. Li H, Yan H. An Analytical Method for Tension Force Estimation of Arch Bridge Suspenders Considering Multiple Factors. Journal of Bridge Engineering. 2024; 29(6). doi: 10.1061/jbenf2.beeng-6594
34. Fujino Y, Kimura K, Tanaka H. Wind Resistant Design of Bridges in Japan. Springer; 2012.
35. Hiroshi Z, Tohru S, Yoshio N, et al. Practical formulas for estimation of cable tension by vibration method. Journal of Structural Engineering. 1996; 122(6): 651-655. doi: 10.1061/(ASCE)0733-9445(1996)122:6(651)
36. Irvine HM, Caughey TK. The linear theory of free vibrations of a suspended cable. Proceedings of the Royal Society of London. A. Mathematical and Physical Sciences. 1974; 341(1626): 299-315. doi: 10.1098/rspa.1974.0189

37. Ministry of Transport of the People's Republic of China. Code for load testing of highway bridges: JTG/T J21-01—2015. Beijing: China Communications Press; 2015.
38. Ren W, Chen G. Practical formula for calculating cable tension based on fundamental frequency. Journal of China Civil Engineering. 2005; 38(11): 26-31.
39. Li H, Shu G, Lu R. Analysis on wind-induced fatigue performance of point-supported glass curtain for flexibly supports system. Steel Construction. 2011; 26: 1-6.